Letter
Vol. 44, No. 21 / 1 November 2019 / Optics Letters 5121
Optics Letters

Low short-wavelength loss fiber Bragg gratings inscribed in a small-core fiber by femtosecond laser point-by-point technology

Xueya Liu,[1,2] Yiping Wang,[1,2,*] Ziliang Li,[1,2] Shen Liu,[1,2] Ying Wang,[1,2] Cailing Fu,[1,2] Changrui Liao,[1,2] Zhiyong Bai,[1,2] Jun He,[1,2] Zhengyong Li,[1,2] and Laipeng Shao[1,2]

[1]Guangdong and Hong Kong Joint Research Centre for Optical Fiber Sensors, College of Physics and Optoelectronic Engineering, Shenzhen University, Shenzhen 518060, China
[2]Key Laboratory of Optoelectronic Devices and Systems of Ministry of Education and Guangdong Province, Shenzhen University, Shenzhen 518060, China
*Corresponding author: ypwang@szu.edu.cn

Received 14 August 2019; revised 22 September 2019; accepted 25 September 2019; posted 27 September 2019 (Doc. ID 375437); published 17 October 2019

A femtosecond-laser-induced fiber Bragg grating (FBG) usually has a higher insertion loss at the shorter wavelength than at the reflection wavelength, i.e., so-called short-wavelength loss. High-quality FBGs are inscribed in different types of small-core single-mode fibers (SMFs) by the use of femtosecond laser point-by-point technology in order to investigate the effect of the fiber core diameter on the grating inscription efficiency and on the short-wavelength loss. A lower laser pulse energy is required to achieve the same grating reflectivity in a smaller-core fiber than in a large-core fiber. The short-wavelength loss of the small-core FBG is lower than that of the large-core FBG with the same reflectivity. Furthermore, a series of FBGs with a low short-wavelength loss are inscribed in a small-core SMF along the fiber axis to achieve so-called series-integrated FBGs (SI-FBGs). Finally, the effect of the input light direction on the reflection peak of the SI-FBGs is investigated to reduce the influence of the grating short-wavelength loss in the sensing and communication applications.

https://doi.org/10.1364/OL.44.005121

An ultraviolet laser phase mask method is usually used to write a fiber Bragg grating (FBG) in a photosensitive optical fiber [1–3]. However, such a method requires an expensive phase mask and is only written one type of FBGs with the same grating pitch [4]. Recently, femtosecond laser inscription has attracted widespread interest and can be used to write various FBGs in almost all types of optical fibers with or without a photosensitivity [5–7]. Moreover, FBGs with different grating pitches can be inscribed by use of the femtosecond laser point-by-point (PbP) technology, and no phase mask is required to achieve an FBG [8,9]. Unfortunately, the femtosecond-laser-induced FBG usually has a high insertion loss at the shorter wavelength than at the reflection wavelength, i.e., so-called short-wavelength loss due to diffractive Mie scattering [10–17], which could be remedied by addressing the overlap integral between the grating and the incident mode by changing the grating size and morphology [10]. Such a high short-wavelength loss is a disadvantage to the communication and sensing applications of the femtosecond-laser-inscribed FBGs.

In this Letter, a high-quality FBG with a very low short-wavelength loss of less than 0.07 dB and a reflectivity of approximately 18.70% was successfully inscribed in a small-core single-mode fiber (SMF) by use of the femtosecond laser PbP technology. Moreover, a series of FBGs with a low short-wavelength loss were inscribed in a small-core SMF along the fiber axis to achieve so-called series-integrated FBGs (SI-FBGs). In addition, the effect of the input light direction on the reflection peak of the SI-FBGs is investigated to reduce the influence of the grating short-wavelength loss.

In our experiments, an experimental setup illustrated in Fig. 1 in Ref. [18] was employed to inscribe low short-wavelength loss FBGs in a few SMFs with different core diameters by use of the femtosecond laser PbP technology and to investigate the effect of the fiber core diameter on the grating inscription efficiency. The femtosecond laser (Spectra-Physics, Solstice) employed has a pulse width of 100 fs, a central wavelength of 800 nm, and a repetition rate of 1 kHz. The laser energy can be adjusted by rotating a half-wave plate with respect to a subsequent Glan–Laser polarizer. A shutter (Thorlabs, Inc., SH05) is mounted in the light path to switch the laser beam on/off. The femtosecond laser, shutter, rotators, and 3D translation stage are simultaneously controlled to inscribe an FBG in an optical fiber by a computer.

To investigate the effect of the fiber core diameter on the grating inscription efficiency, three FBGs with a grating pitch of 1.070 μm and a grating length of 2 mm were successfully inscribed in three types of SMFs with a core diameter of 9.0, 5.1, and 4.4 μm, by the femtosecond laser PbP technology. Note that the fiber coating was not stripped off before an FBG is inscribed. The pulse energy of the femtosecond laser

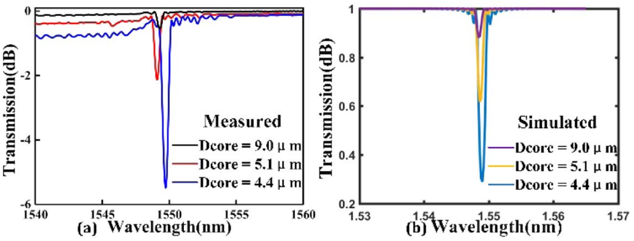

Fig. 1. (a) Measured and (b) simulated transmission spectra of three FBGs inscribed in three types of SMFs with a core diameter of 9.0, 5.1, and 4.4 μm.

employed is 142 nJ. As shown in Fig. 1(a), the measured resonant efficiency of the three FBGs is 0.545, 2.135, and 5.481 dB. In other words, the FBG inscription efficiency in a smaller-core SMF is higher than that in a larger-core SMF. As shown in Fig. 1(b), we also simulated transmission spectra of the three FBGs to investigate the dependence of the grating resonance on the fiber core. The simulated transmission spectrum of each FBG is almost the same as the measured transmission spectrum. It can be seen from Fig. 1(a) that each FBG has an obvious insertion loss at a shorter wavelength than at the reflection wavelength.

Depending on laser, focusing, and material parameters, different refractive index modulation mechanisms, e.g., small density, color centers, and microvoids, may play a role in the femtosecond-laser-inscribed FBGs [14,15]. During our grating inscriptions, the laser beam with a pulse energy of 142 nJ was focused on the fiber core by use of an oil-immersion microscope objective with an NA value of 1.25. As a result, a microvoid with a small diameter of approximately 1 μm and a large densified region occurs in the fiber core due to the high-energy pulse-induced microexplosion [19]. The densification is initially negligible, and only the microvoid is evaluated for refractive index modulation. This is reasonable since the index change of the microvoid is at least one order of magnitude greater than that of the densification [20]. As shown in Fig. 2, the ratio of the microvoid size (red) to the fiber core size (gray) in a small-core fiber is higher than that in a large-core fiber. Thus, the microvoid-induced refractive index change in a small-core fiber is higher than that in a large-core fiber. Therefore, the same pulse energy induced a stronger resonant coupling in the small-core (4.4 μm) fiber than in the large-core (5.1 or 9.0 μm) fiber, as shown in Fig. 1. In other words, the grating inscription efficiency is higher in a small-core fiber than that in a large-core fiber, while the femtosecond laser PbP technology is employed to inscribe an FBG.

To further investigate the effect of the fiber core diameter on the short-wavelength loss, as shown in Figs. 3 and 4, four FBGs with almost the same reflectivity of approximately 20% were inscribed in four types of SMFs with a core diameter of 9.0, 5.1, 4.4 and 1.8 μm by use of the femtosecond laser PbP technology. Note that different laser pulse energies of 174, 124, 98, and 59 nJ were employed to achieve almost the same grating reflectivity in the four FBGs, i.e., FBG_1, FBG_2, FBG_3, and FBG_4, with a core diameter of 9.0, 5.1, 4.4, and 1.8 μm, respectively. As shown in Fig. 3, the short-wavelength loss of an FBG inscribed in a smaller-core SMF is much lower than that of an FBG inscribed in a larger-core SMF. For example, the measured insertion loss of FBG_1, FBG_2, FBG_3, and FBG_4 at a shorter wavelength than the reflection wavelength, e.g., 1525 nm, is −0.592, −0.438, −0.313, and −0.063 dB, respectively.

As shown in Fig. 4, obvious microvoids, i.e., periodic white spots, were observed on the core of the femtosecond-laser-induced FBGs. The microvoid size is significantly smaller than the modes of the waveguides and, therefore, should be prone to significant Mie scattering [11,12]. Consequently, as shown in Fig. 3, such microvoids induce strong and permanent attenuation at a short wavelength due to diffractive Mie scattering, which can only be remedied by addressing the overlap integral between the grating and the incident mode by changing the grating size and morphology [10,21]. As described above, the same pulse energy induced a stronger resonant coupling in a small-core fiber than in a large-core fiber. Thus, a lower laser pulse energy is required to achieve the same grating reflectivity in a small-core fiber than in a large-core fiber. Furthermore, the lower the laser pulse energy, the lower is the microvoid-induced short-wavelength loss due to diffractive

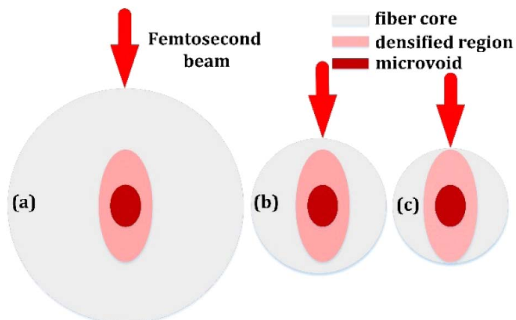

Fig. 2. Schematic diagram of the fiber core, densified region, and microvoid on the cross section of a SMF with a core diameter of (a) 9.0, (b) 5.1, and (c) 4.4 μm, respectively.

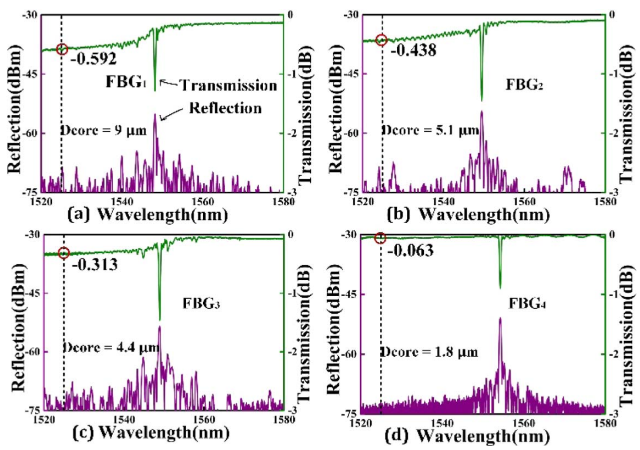

Fig. 3. Transmission (green) and reflection (purple) spectra of the four FBGs, i.e., FBG_1, FBG_2, FBG_3, and FBG_4, with almost the same reflectivity of 20% inscribed in four types of SMFs with a core diameter of (a) 9.0, (b) 5.1, (c) 4.4, and (d) 1.8 μm, respectively. The four FBG samples have the same grating pitch of 1.070 μm, the same grating length of 2 mm, and almost the same resonance wavelength of 1550 nm.

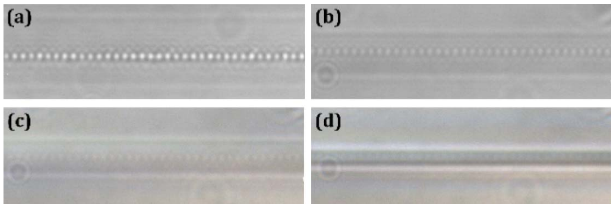

Fig. 4. Microscope images of the four FBGs, i.e., FBG_1, FBG_2, FBG_3, and FBG_4, with almost the same reflectivity of 20% inscribed in four types of SMFs with a core diameter of (a) 9.0, (b) 5.1, (c) 4.4, and (d) 1.8 μm, respectively.

Mie scattering. Therefore, the short-wavelength loss of the small-core FBG is lower than that of the large-core FBG with the same reflectivity, as shown in Fig. 3.

As shown in Fig. 1, the short-wavelength loss of the FBG inscribed in a smaller-core fiber is higher than that of the FBG inscribed in a larger-core fiber. The reason for this is that the same laser pulse energy of 142 nJ was employed to inscribe FBGs in the three types of SMFs with a core diameter of 9.0, 5.1, and 4.4 μm, so that microvoids with a similar size were formed in the core of the three optical fibers. As shown in Fig. 2, the ratio of the microvoid size (red) to the fiber core size (gray) in a small-core fiber is higher than that in a large-core fiber. Therefore, the microvoid-induced short-wavelength loss, resulting from diffractive Mie scattering, in an FBG inscribed in a small-core fiber is higher than that in another FBG in a large-core fiber, and a stronger resonant coupling occurs in an FBG inscribed in a small-core fiber, rather than in another FBG inscribed in a large-core fiber.

To investigate the applications of our low-loss FBGs in the field of optical fiber sensors, especially distributed optical fiber sensors, a series of FBGs, i.e., SI-FBGs, were gradually inscribed in the core of an optical fiber along the fiber axis by use of the femtosecond laser PbP technology. For example, 10 FBGs, i.e., $FBG_1, FBG_2, \ldots,$ and FBG_{10}, with a grating pitch of 1.01, 1.02, …, and 1.10 μm, respectively, were gradually inscribed in a small-core SMF (CS980/125-16/250) with a core diameter of 4.4 μm, as shown in Fig. 5(a). The spacing between two FBGs is about 2 mm along the fiber axis. An optical spectrum analyzer (Model AQ6370C, Yokogawa Electric Corp., Japan) with a resolution of 0.05 nm and a broadband amplified spontaneous emission light source (BBS, Fiber Lake ASE-Light-Source, Shenzhen, China) with a wavelength range from 1450 to 1625 nm were employed to measure transmission spectra of the 10 SI-FBGs. As shown in Fig. 5(b), each FBG inscribed in the small-core SMF has an insertion loss of about 0. 25 dB at the wavelength of 1450 nm, and a total insertion loss of the 10 FBGs is approximately 2.5 dB at the wavelength of 1450 nm.

To investigate the effect of the input light direction on the reflection peak of SI-FBGs, the reflection spectra of the 10 SI-FBGs were measured, while light was input from the FBG_1 end to the FBG_{10} end or from the opposite direction. As shown in Fig. 6 and Table 1, while light was input from the FBG_1 end to the FBG_{10} end; the reflection peak of each FBG is −51.616, −50.443, −46.553, …, and −46.646 dBm, respectively. In contrast, while light was input from the FBG_{10} end to the FBG_1 end; the reflection peak of each FBG is

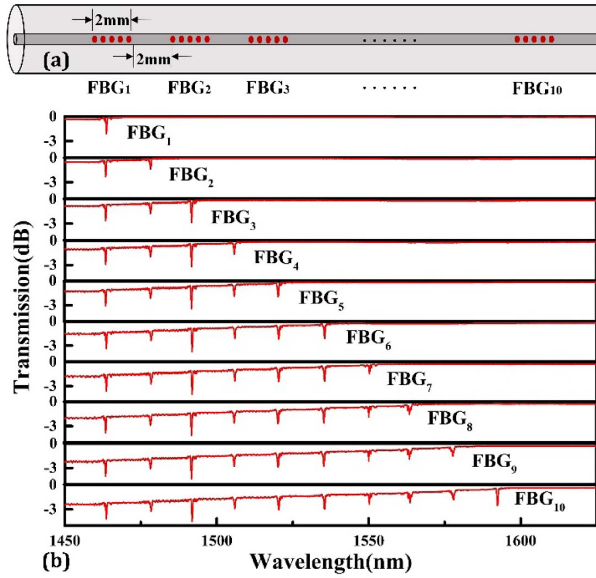

Fig. 5. (a) Schematic diagram and (b) transmission spectra of the SI-FBGs with a grating length of 2 mm inscribed in a SMF with a core diameter of 4.4 μm. The spacing between two FBGs is about 2 mm.

−56.533, −54.383, −50.375, …, and −46.126 dBm, respectively. The difference of each FBG reflection peak between the two opposite input light directions is 4.917, 3.940, 3.822, …, and −0.520 dB, respectively, as shown in Table 1.

The reason for this is that, while light was input from the FBG_{10} end to the FBG_1 end, the reflected light of an FBG, e.g., FBG_i ($i = 1, 2, \ldots, 9$), with a shorter reflection wavelength will be decayed by other FBGs, e.g., $FBG_{i+1}, FBG_{i+2}, \ldots,$ and FBG_{10}, with a longer reflection wavelength due to their short-wavelength loss. In contrast, while light was input from the FBG_1 end to the FBG_{10} end, the reflected light of an FBG, e.g., FBG_i ($i = 2, 3, \ldots, 10$) with a longer reflection wavelength will not be decayed by the short-wavelength loss of other FBGs, e.g., $FBG_{i-1}, FBG_{i-2}, \ldots,$ and FBG_1 with a shorter reflection wavelength, but it will be decayed by the insertion loss of other FBGs at a longer wavelength, i.e., so-called the long-wavelength loss. In addition, the short-wavelength loss of each femtosecond-laser-inscribed FBG is much higher than the long-wavelength loss. Therefore, the reflection peaks of the SI-FBGs depend strongly on the input light direction. Thus,

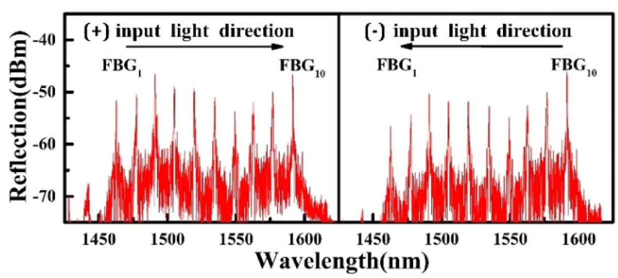

Fig. 6. Reflection spectra of the 10 SI-FBGs inscribed in a SMF with a core diameter of 4.4 μm, while the input light propagates along the '+' direction (from FBG_1 to FBG_{10}) or the '-' direction (from FBG_{10} to FBG_1).

Table 1. Measured Peak Reflections of the 10 SI-FBGs and the Difference of each FBG Reflection Peak Between the Two Opposite Input Light Directions

Input Light Propagating Direction	FBG_1	FBG_2	FBG_3	FBG_4	FBG_5	FBG_6	FBG_7	FBG_8	FBG_9	FBG_{10}
'+': $FBG_1 \rightarrow FBG_{10}$ (Unit: dBm)	−51.616	−50.443	−46.553	−48.953	−49.265	−51.035	−53.769	−51.985	−49.994	−46.646
'-': $FBG_1 \leftarrow FBG_{10}$ (Unit: dBm)	−56.533	−54.383	−50.375	−51.851	−51.796	−52.776	−54.902	−52.573	−50.059	−46.126
'+'—'-'(Unit: dB)	4.917	3.940	3.822	2.898	2.531	1.741	1.133	0.588	0.065	−0.520

in the applications of the SI-FBGs, light should be input from an FBG with a shorter reflection wavelength to another FBG with a longer reflection wavelength in order to reduce the influence of the short wavelength.

In conclusion, a high-quality FBG with a very low short-wavelength loss was successfully inscribed in a small-core SMF by use of the femtosecond laser PbP technology. In addition, a lower laser pulse energy is required to achieve the same grating reflectivity in a small-core fiber than in a large-core fiber. The short-wavelength loss of the small-core FBG is lower than that of the large-core FBG with the same reflectivity. For example, the four FBGs with a core diameter of 9.0, 5.1, 4.4, and 1.8 μm, were inscribed by employing a laser pulse energy of 174, 124, 98, and 59 nJ, respectively, and exhibited a short-wavelength loss of −0.592, −0.438, −0.313, and −0.063 dB, respectively, at the wavelength of 1525 nm. Moreover, a series of SI-FBGs were inscribed in the fiber core along the fiber axis. The reflection peaks of the SI-FBGs depend strongly on the input light direction. In the applications of the SI-FBGs, light should be input from an FBG with a shorter reflection wavelength to another FBG with a longer reflection wavelength in order to reduce the influence of the short wavelength.

Funding. National Natural Science Foundation of China (61635007, 61705138); Science and Technology Innovation Commission of Shenzhen (JCYJ20170412105604705); Development and Reform Commission of Shenzhen Municipality Foundation; Natural Science Foundation of Guangdong Province (2017A030310033).

REFERENCES

1. K. O. Hill, B. Malo, F. Bilodeau, D. C. Johnson, and J. Albert, Appl. Phys. Lett **62**, 1035 (1993).
2. P. J. Lemaire, R. M. Atkins, V. Mizrahi, and W. A. Reed, Electron. Lett. **29**, 1191 (1993).
3. K. O. Hill, Y. Fujii, D. C. Johnson, and B. S. Kawasaki, Appl. Phys. Lett **32**, 647 (1978).
4. K. O. Hill and G. Meltz, J. Lightwave Technol. **15**, 1263 (1997).
5. K. K. T. Geernaert, C. Koutsides, M. Komodromos, W. U. T. Nasilowski, J. Wojcik, F. Berghmans, and H. Thienpont, Opt. Lett. **35**, 1647 (2010).
6. J. Thomas, C. Voigtländer, R. G. Becker, D. Richter, A. Tünnermann, and S. Nolte, Laser Photonics Rev. **6**, 709 (2012).
7. A. M. Y. Lai, I. Khrushchev, and I. Bennion, Opt. Lett **31**, 1672 (2006).
8. A. Martinez, I. Y. Khrushchev, and I. Bennion, Opt. Lett **31**, 1603 (2006).
9. K. Z. Y. Lai, K. Sugden, and I. Bennion, Opt. Express **15**, 18318 (2007).
10. N. J. Mattias, L. Åslund, N. Groothoff, J. Canning, G. D. Marshall, S. D. Jackson, A. Fuerbach, and M. J. Withford, Opt. Express **16**, 14248 (2008).
11. P. C. Hill, G. R. Atkins, J. Canning, G. C. Cox, and M. G. Sceats, Appl. Opt. **34**, 7689 (1995).
12. V. Mizrahi and J. E. Sipe, J. Lightwave Technol. **11**, 1513 (1993).
13. S. M. Eaton, H. Zhang, J. Li, and P. R. Herman, Opt. Lett **31**, 3495 (2006).
14. M. D. Amos Martinez, I. Khrushchev, and I. Bennion, IEEE Photonics Technol. Lett. **18**, 2266 (2006).
15. C. B. Schaffer, A. O. Jamison, and E. Mazur, Appl. Phys. Lett. **84**, 1441 (2004).
16. R. J. Williams, N. Jovanovic, G. D. Marshall, G. N. Smith, M. J. Steel, and M. J. Withford, Opt. Express **20**, 13451 (2012).
17. J. N. Thomas, R. G. Becker, G. D. Marshall, M. Withford, A. Tünnermann, S. Nolte, and M. J. Steel, Opt. Express **19**, 325 (2011).
18. C. Zhang, Y. Yang, C. Wang, C. Liao, and Y. Wang, Opt. Express **24**, 3981 (2016).
19. E. N. Glezer and E. Mazur, Appl. Phys. Lett **71**, 882 (1997).
20. J. T. N. Jovanovic, R. J. Williams, M. J. Steel, G. D. Marshall, A. Fuerbach, S. Nolte, A. Tünnermann, and M. J. Withford, Opt. Express **17**, 6082 (2009).
21. A. Othonos, Rev. Sci. Instrum. **68**, 4309 (1997).